J Porous Mater (2018) 25:621–627
DOI 10.1007/s10934-017-0475-1

Highly porous carbons obtained by activation of polypyrrole/reduced graphene oxide as effective adsorbents for CO_2, H_2 and C_6H_6

Barbara Szczęśniak[1] · Łukasz Osuchowski[2] · Jerzy Choma[1] · Mietek Jaroniec[3]

Published online: 14 July 2017

Abstract A series of highly porous carbon materials has been prepared from polypyrrole/reduced graphene oxide composite by one step carbonization and activation process. Two activation agents were used in this study potassium hydroxide and potassium citrate. The resulting samples exhibited high BET surface areas ranging from 1650 to 2780 m^2/g, large total pore volumes in the range of 0.73–1.66 cm^3/g, and high micropore volumes in the range of 0.43–0.78 cm^3/g. The most porous material was synthesized by using KOH impregnation and featured hydrogen adsorption capacity of 11.3 mmol/g (2.3 wt% H_2) at −196 °C under 760 mmHg and C_6H_6 capacity of 15.8 mmol/g at 20 °C and pressure close to the saturation vapor pressure. Also, highly ultramicroporous carbon was obtained by activation of the aforementioned composite with potassium citrate, which was confirmed by very high adsorption (6.8 mmol/g) of CO_2 at 0 °C and 760 mmHg. The excellent adsorption properties of the synthesized carbons for CO_2, H_2 and benzene vapor were achieved by adjusting activation procedure specifically for each adsorbate used.

Keywords Gas adsorption · Benzene vapor · Hydrogen · Carbon dioxide · Polymer/graphene composite · Highly porous sorbents

1 Introduction

A continuous industrial growth is associated with rising energy demands and emission of hazardous gases into atmosphere. These negative effects of industrial development can be diminished by reducing emissions of CO_2 and other hazardous gases to atmosphere and searching for sustainable energy sources such as H_2 or CH_4. However, the generation and storage of these fuels are challenging tasks. The U.S. Department of Energy established targets for onboard hydrogen storage systems for light-duty fuel cell vehicles: 0.055 kg H_2/kg system for the gravimetric capacity and 0.040 kg H_2/L system for the volumetric capacity [1].

Many various materials have been proposed as potential gas adsorbents for commercial applications. Among them activated carbons, metal organic frameworks (MOFs) and graphene materials have attracted a lot of attention; for instance, MOF-210 adsorbed 54.5 mmol CO_2/g at 25 °C and 50 bar [2]. In comparison, polyaniline-modified graphene material adsorbed 75 mmol CO_2/g at 25 °C and under lower pressure (11 bar) [3]. Activated carbons are among the best CO_2 adsorbents at ambient conditions [4–6]. For instance, Wickramaratne and Jaroniec [4] reported the CO_2 uptake of 8.9 mmol/g at 0 °C and 1 atm for phenolic resin-derived activated carbons. MOFs are considered as potential storage materials for hydrogen, mainly because of their large BET specific surface areas up to ~7000 m^2/g; for instance, MOF-174-Mg showed H_2 uptake of 4.33 wt% at −196 °C and 20 bar [7].

Electronic supplementary material The online version of this article (doi:10.1007/s10934-017-0475-1) contains supplementary material, which is available to authorized users.

✉ Mietek Jaroniec
jaroniec@kent.edu

[1] Institute of Chemistry, Military Technical Academy, 00-908 Warsaw, Poland

[2] Military Institute of Chemistry and Radiometry, 00-910 Warsaw, Poland

[3] Department of Chemistry and Biochemistry, Kent State University, Kent, OH 44-242, USA

Activated graphene-based materials also exhibit great gas adsorption properties. A KOH activated graphene oxide (a-rGO) was shown to be very efficient H_2 adsorbent [8]. This material adsorbed 7.0 wt% H_2 at −196 °C under 40 bar and 4.2 wt% H_2 at −80 °C under 120 bar. Nevertheless, a key drawback of the proposed synthesis method is low efficiency—up to 80% loss during activation process. Other activated graphene material had BET specific surface area of 3240 m^2/g and showed high gas adsorption for various gases: H_2—3.8 wt% (196 °C, 10 bar), CH_4—11.3 mmol/g (25 °C, 35 bar), CO_2—21 mmol/g (25 °C, 20 bar) [9]. Various activation routes have been explored to develop highly porous graphene materials. Among them, KOH activation was shown to be a very effective route.

It is noteworthy that many effective sorbents were obtained from polymers or waste polymeric materials [10, 11]. Furthermore, composite sorbents obtained by coupling graphene oxide with polymers (e.g., polypyrrole, polyethyleneimine, polyindol) were shown to be effective adsorbents, especially at ambient conditions [12–14]. Much less attention has been devoted to the development of sorbents for volatile organic compounds (VOCs) [15–17]. Benzene, one of the most common VOCs, is commonly used in the chemical industry as a substrate in organic synthesis and also as a high-energy component of gasoline. Benzene is a subject of air quality assessment because of its well-documented carcinogenicity [18]. Thus, there is an ongoing search for effective adsorbents for benzene vapor and other VOCs. Unfortunately, experimental studies devoted to benzene adsorption are rare, mainly due to the harmfulness of benzene and time-consuming complex measurements. While highly microporous carbons (with pores below 1 nm) are best suited for CO_2 adsorption at ambient conditions, high benzene uptake can be achieved for sorbents with large volume of larger micropores and small mesopores [15, 19]. The above mentioned studies indicate that there are still great opportunities in the development of new, highly microporous composites for sorption of various gases such as CO_2, H_2 and C_6H_6 by merging polypyrrole with graphene or graphene oxide followed by specially designed activation that generates porosity suitable for the adsorbate used. This topic is discussed in the current work.

2 Experimental

2.1 Chemicals

All chemicals were purchased and used without further purification. Graphite powder (99.99%), potassium permanganate (99.5%), hydrogen peroxide (30%), sulfuric acid (95%), orthophosphoric acid (85%), pyrrole (99.8%), ammonium persulfate (98%), hydrazine monohydrate (80%), potassium hydroxide (85%), potassium citrate monohydrate (99%), hydrochloric acid (35%) and hydrofluoric acid (40%).

2.2 Synthesis of graphite oxide

Graphite oxide was synthesized from graphite powder using a modified Hummer's method [20, 21]. In brief, 1.5 g of graphite powder was mixed with 9 g of $KMnO_4$ and added slowly to a mixture of concentrated H_2SO_4 (180 mL) and H_3PO_4 (20 mL) under stirring. The mixture was than heated to 50 °C and stirred for 12 h. After cooling, it was poured onto ice (~200 mL) with 3 mL of 30% H_2O_2. Finally, the supernatant was washed copiously with deionized water (DI H_2O) by centrifugation and dried under vacuum at 40 °C.

2.3 Synthesis of polypyrrole/reduced graphene oxide

Synthesis of polypyrrole/reduced graphene oxide composite (PPy/rGO) was performed according to the procedure reported by Chandra et al. [12]. In brief, 250 mg of graphite oxide and 1 g of pyrrole were dispersed in 100 mL of DI H_2O. Next, 4 g of $(NH_4)_2S_2O_8$ was added to the above mixture and polymerization was conducted for 12 h. The last step in the synthesis of PPy/rGO composite involved reduction of GO with 2.5 mL of $N_2H_4{\cdot}H_2O$ at 90 °C. Reduced graphene oxide (rGO) without polypyrrole was also prepared.

2.4 Activation of PPy/rGO

Firstly, PPy/rGO was impregnated with 7 M KOH aqueous solution for 24 h. Secondly, after drying it was heated in flowing nitrogen in a tubular furnace at 600–800 °C for 1 h. Thirdly, the resulting material was washed with 8% HCl and next treated with 20% HF in an ultrasonic bath for 5 min. Finally, the product was washed with DI H_2O and dried under vacuum at 70 °C to obtain PPy/rGO-KOHx (x denotes the activation temperature in °C). KOH activated rGO was also prepared using the same activation route; the resulting sample was labeled as rGO-KOH700. Additionally, one sample was obtained using potassium citrate as an activation agent. In this case, prior to heating at 700 °C for 1 h in nitrogen flow, PPy/rGO was simply mixed with solid potassium citrate (1:4 PPy/rGO:K weight ratio). Next, the same washing and drying procedures as described above were applied. The product was denoted as PPy/rGO-Cit700.

2.5 Characterization methods

Scanning electron microscopy (SEM), Raman spectroscopy (RS) and X-ray diffraction (XRD) analysis were used

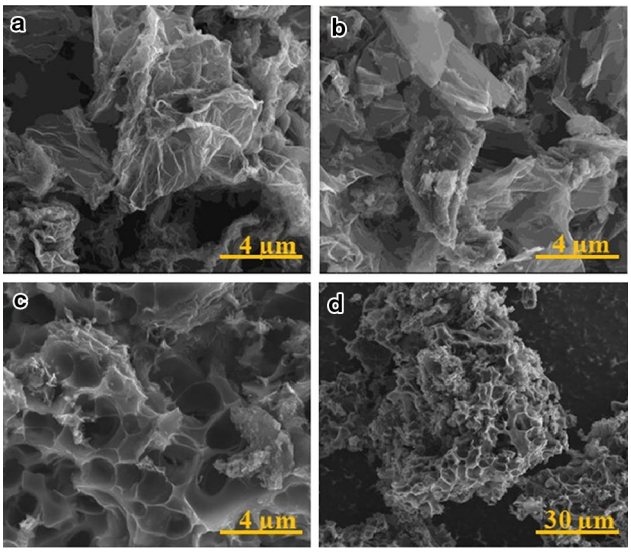

Fig. 1 SEM images of rGO (**a**), PPy/rGO (**b**), and PPy/rGO-KOH700 (**c, d**)

Table 1 Elemental composition (at.%) of rGO, PPy/rGO and PPy/rGO-KOH700

Element	Concentration (at.%)		
	rGO	PPy/rGO	PPy/rGO-KOH700
C	83.39	76.53	87.28
N	3.26	8.79	2.06
O	12.73	14.14	10.35
S	0.02	0.34	0.04
Al	0.08	0.08	0.06
Si	0.06	0.05	0.06
Cl	0.01	0.07	0.04
Ca	0.03	–	–
Ce	0.05	–	–
Mn	0.36	–	–
K	–	–	0.05
Fe	–	–	0.01
Ni	–	–	0.03

to characterize morphology and structure of the rGO, PPy/rGO and PPy/rGO-KOH700 samples. The elemental composition analysis of the samples was performed by energy dispersive spectroscopy method using a FEI Quanta 3D FEG scanning electron microscope equipped with silicon drift detector. RS was conducted on a Renishaw inVia Reflex instrument using 514 nm laser. XRD analysis was carried out on a PANalytical Empyrean diffractometer with Cu Kα X-rays operating at 40 V and 30 mA. Adsorption of N_2 and H_2 was measured at −196 °C and CO_2 at 0 °C using a volumetric adsorption analyzer ASAP 2020 manufactured by Micromeritics Instrument Corp. (Norcross, GA, USA). Benzene adsorption at 20 °C was measured using McBain–Bakr gravimetric method on a home-made apparatus equipped with a quartz-spring balance. Each graphene-based sample was degassed in a vacuum at 100 °C for 24 h prior to adsorption measurements.

3 Results and discussion

Figure 1 shows SEM images of rGO, PPy/rGO and PPy/rGO-KOH700. The images of rGO and PPy/rGO show clearly graphene layers. PPy/rGO-KOH700 shows rather irregular macroporosity (pores above 50 nm) with incorporated highly defected, stacked graphene layers. Table 1 provides the elemental composition (at.%) of the samples. Atomic concentrations in the samples indicate a partial oxidation of graphene surface and trace amounts of impurities. It is noteworthy, that rGO and PPy/rGO show relatively small content of oxygen up to 14.14 at.%. After activation of PPy/rGO the oxygen concentration was further reduced to 10.35 at.%, while nitrogen concentration was reduced from 8.79 to 2.06 at.%.

The XRD pattern (Fig. 2) shows the (002) diffraction peak at 2θ = 24.59° (rGO), 2θ = 25.87° (PPy/rGO) and 25.52° (PPy/rGO-KOH700) indicating the interlayer distances of 0.36 nm (rGO), 0.34 nm (PPy/rGO) and 0.35 nm (PPy/rGO-KOH700). The (10) diffraction peak at 2θ = 43.16° (rGO), 2θ = 42.95° (PPy/rGO) and 43.52° (PPy/rGO-KOH700) reflects a short range order in stacked graphene layers [22]. This peak is clearly visible for rGO indicating the best ordered structure among the analyzed samples. The Raman spectra of rGO, PPy/rGO and PPy/rGO-KOH700 show intensive D and G bands. The D band is attributed to defects or disorder. High intensity D band (1356 cm^{-1}) in rGO suggests that defects were induced in graphite by oxidation and reduction. The 2D band is the second order of the D band, often referred to as an overtone of the D band. The G band correspond to the sp^2 carbon atoms. The G band of rGO is located at 1592 cm^{-1}, while that of PPy/rGO-KOH700 is shifted back to 1586 cm^{-1} indicating further reduction of rGO during heating up to 700 °C.

Figure 3 shows the low-temperature nitrogen adsorption–desorption isotherms measured for all samples; additional semi-logarithmic graph of these isotherms is shown in the supporting information as Fig. 1S. Figure 4 displays the corresponding pore size distribution functions (PSDs) for activated composite samples. These PSD functions were calculated based on the low-temperature nitrogen adsorption using the non-local density functional theory method (2D-NLDFT) for carbon slit-shaped pores by taking into

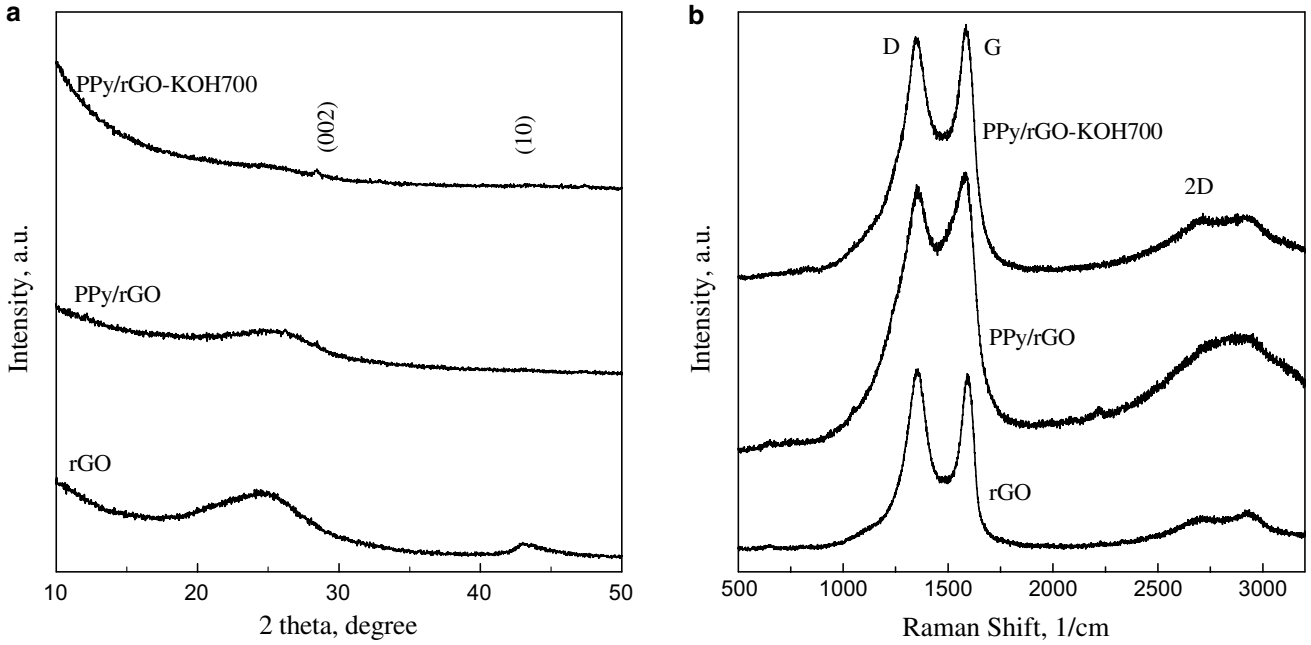

Fig. 2 XRD pattern (**a**) and Raman spectra (**b**) of rGO, PPy/rGO and PPy/rGO-KOH700

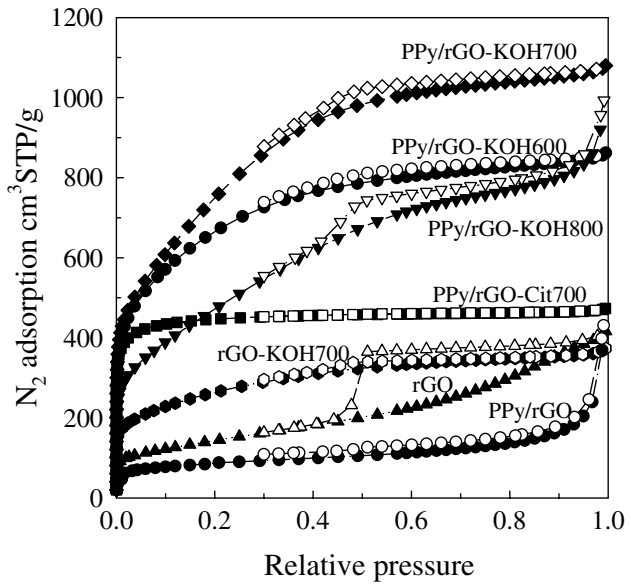

Fig. 3 Low-temperature (−196 °C) N_2 adsorption–desorption isotherms measured on all graphene-based materials

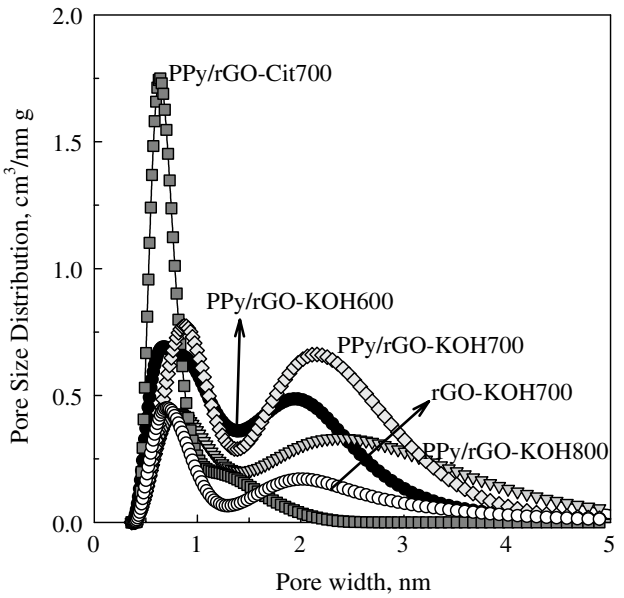

Fig. 4 Differential pore size distribution functions calculated for all activated samples

account energetic heterogeneity and geometrical corrugation of the surface [23, 24]. The specific surface area (S_{BET}) was calculated using Brunauer–Emmett–Teller method based on the nitrogen isotherms in a relative pressure range of 0.05–0.2 [25]. The total pore volume (V_t) was calculated using volume of nitrogen adsorbed at $p/p_0 \approx 0.99$. Table 2 shows the structural parameters listed for all samples. The activated composite samples feature high specific surface areas varying from 940 to 2780 m^2g. The highest value of S_{BET} (2780 m^2/g) and V_t (1.66 cm^3/g) was obtained for the composite sample activated with KOH at 700 °C (PPy/rGO-KOH700) (Table 2). This study shows that KOH activation at 700 °C was optimal for achieving high micro-mesoporosity in PPy/rGO. It should be mentioned that the higher activation temperature reduces the efficiency of activation

Table 2 Structural parameters of all samples

Graphene material	S_{BET} (m^2/g)	V_t (cm^3/g)	V_{ultra} (cm^3/g)	V_{micro} (cm^3/g)	Microporosity (%)
rGO	510	0.63	0.04	0.12	19
PPy/rGO	290	0.67	0.02	0.10	15
rGO-KOH700	940	0.57	0.08	0.30	53
PPy/rGO-KOH600	2270	1.33	0.14	0.78	59
PPy/rGO-KOH700	2780	1.66	0.07	0.74	45
PPy/rGO-KOH800	1730	1.54	0.05	0.43	28
PPy/rGO-Cit700	1650	0.73	0.31	0.67	92

S_{BET} – BET specific surface area; V_t – total (single-point) pore volume obtained from the amount adsorbed at $p/p_0 \approx 0.99$; V_{ultra} – volume of ultramicropores (pores <0.7 nm) obtained on the basis of DFT PSD; V_{micro} – volume of micropores (pores <2 nm) obtained on the basis of DFT PSD; Microporosity – percentage of volume of micropores (V_{micro}) in the total pore volume (V_t)

process to 45% yield in the case of PPy/rGO-KOH700. Pore size distribution functions well illustrate structural changes upon activation at different temperatures (Fig. 4). We found that lower temperature in the range of 600–800 °C does not over activate samples, which leads to the creation of large micropores and small mesopores. Maxima on the PSD curves calculated for KOH activated materials appear in the following ranges 0.5–0.8 and 2.0–2.5 nm. In general, all the KOH activated materials possess ultramicropores, supermicropores and small mesopores. Whereas potassium citrate activated sample at 700 °C was highly microporous (92%) and had large volume of ultramicropores (0.31 cm^3/g). This shows the importance of activating agent for controlling the range of microporosity in the graphene-based samples.

4 Adsorption of CO_2, H_2 and C_6H_6

Carbon dioxide adsorption isotherms were measured on the most microporous materials (PPy/rGO-KOH600, PPy/rGO-KOH700 and PPy/rGO-Cit700) at 0 °C up to 850 mmHg (Fig. 5); also semi-logarithmic graph of these isotherms is shown in the supporting information as Fig. 2S. The highest CO_2 uptake of 6.8 mmol/g was obtained at 0 °C and 760 mmHg and 4.3 mmol/g at 25 °C and 760 mmHg for PPy/rGO-Cit700 because this material featured the highest fraction of micropores (92%) among all samples studied. At the same conditions PPy/rGO-KOH600 and PPy/rGO-KOH700 adsorbed 5.4 mmol/g and 4.9 mmol/g CO_2, respectively. Ultramicropores (<0.7 nm) are mainly responsible for high CO_2 uptake at ambient pressure due to the enhanced gas–solid interactions inside fine micropores. Further adsorption studies were conducted for H_2 and C_6H_6 on PPy/rGO-KOH700, which possessed the highest surface area (2780 m^2/g). For the purpose of comparison, we also measured C_6H_6 adsorption isotherm on a commercially available metal organic framework—Basolite Z377 labeled as MOF-Zn, which featured very high

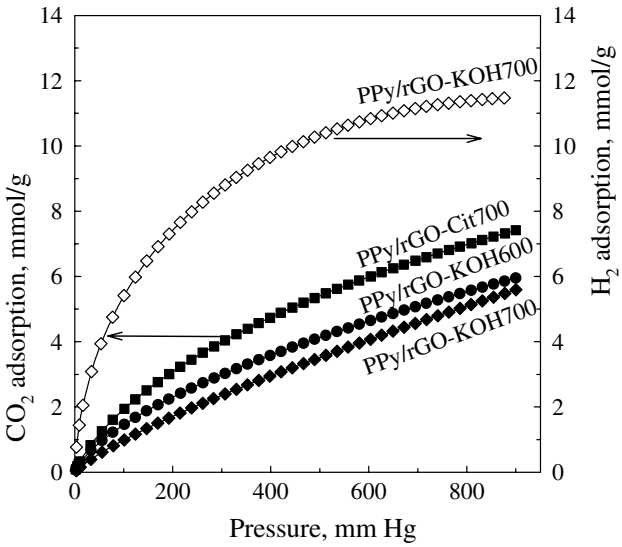

Fig. 5 CO_2 adsorption isotherms measured on the most microporous samples (PPy/rGO-Cit700, PPy/rGO-KOH600, PPy/rGO-KOH700) at 0 °C and H_2 adsorption isotherm measured on PPy/rGO-KOH700 at −196 °C

surface area (~3800 m^2/g). Figure 5 shows H_2 adsorption isotherm measured on PPy/rGO-KOH700 at −196 °C up to 850 mmHg and Fig. 6 shows C_6H_6 adsorption isotherms measured on PPy/rGO-KOH700 and MOF-Zn at 20 °C and relative pressure p/p_0 close to unity. The graphene material exhibited great affinity toward H_2—11.3 mmol/g (2.3 wt%) at −196 °C under 760 mmHg and C_6H_6—15.8 mmol/g at 20 °C and $p/p_0 \sim 1$. Note that PPy/rGO-KOH700 shows only a slightly smaller C_6H_6 uptake (~1 mmol/g) at $p/p_0 \sim 1$ despite its much smaller specific surface area (~1000 m^2/g) as compared to that of MOF-Zn. High C_6H_6 uptake on PPy/rGO-KOH700 was achieved due to its micro-mesoporous structure with small mesopores (2–5 nm). This result agrees well with previous studies of benzene adsorption on activated carbons at ambient conditions [19]; benzene

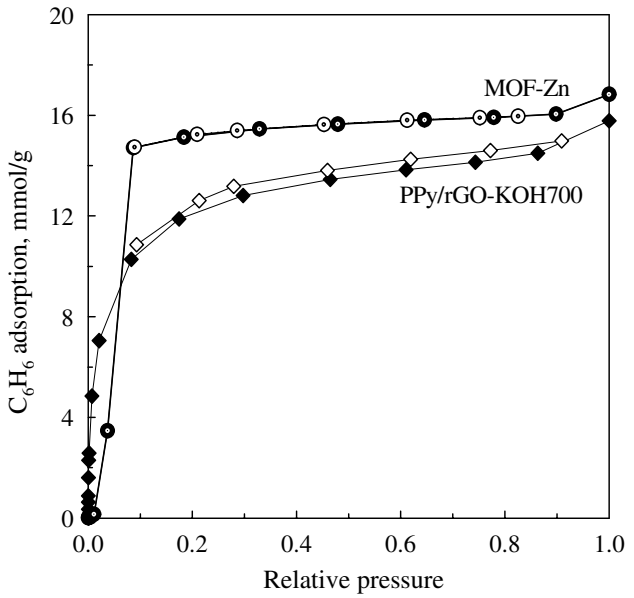

Fig. 6 C_6H_6 adsorption isotherms measured on PPy/rGO-KOH700 and MOF-Zn at 20 °C

Table 3 Adsorption uptakes for CO_2, H_2, at 760 mmHg and C_6H_6 at a pressure close to the saturation vapor pressure on activated polypyrrole/graphene composites

Composite sorbent	CO_2 (mmol/g) T = 0 °C	H_2 (mmol/g) T = −196 °C	C_6H_6 (mmol/g) T = 20 °C
PPy/rGO-KOH600	5.4	–	–
PPy/rGO-KOH700	4.9	11.3	15.8
PPy/rGO-Cit700	6.8	–	–

mainly adsorbs in micropores and small mesopores through volume filling mechanism. Table 3 provides CO_2, H_2, and C_6H_6 adsorption data measured on PPy/rGO-KOH700 and additionally CO_2 adsorption on PPy/rGO-KOH600 and PPy/rGO-Cit700.

To obtain the KOH activated samples we used a slightly modified procedure proposed by Chandra et al. [12], which resulted in composite samples of tailorable structural parameters that are well suited for adsorption of CO_2 at 0 °C and 760 mmHg, H_2 adsorption at −196 °C, or adsorption of benzene vapor at 20 °C. Treatment of the activated materials with 20% HF (a special caution recommended in experiments involving HF) in an ultrasonic bath was a key to highly develop porosity of the samples. KOH activated polypyrrole/graphene composite reported in ref [12] was microporous ($V_t = 0.59$ cm^3/g, $S_{BET} = 1360$ m^2/g) and able to capture 4.3 mmol/g CO_2 at 25 °C and 760 mmHg. No further adsorption measurements (toward H_2 or C_6H_6) were conducted for this adsorbent. In our work, to achieve highly microporous structure we used solid potassium citrate as an activation agent of the polypyrrole/graphene composite, instead of the corrosive, harmful base. The as-prepared sample (PPy/rGO-Cit700) adsorbed the same amount of CO_2 (4.3 mmol/g) at ambient conditions (25 °C, 760 mmHg) as above mentioned adsorbent obtained by the another group [12]. This indicates that KOH can be successfully replaced by an environmentally friendly chemical such as potassium citrate. Furthermore, the adsorption data obtained for PPy/rGO-KOH700 are competitive to those reported for other graphene materials. For instance, nanoporous graphene material reported by Chowdhury and Balasubramanian [26] and N-doped graphene aerogel reported by Sui et al. [27] exhibited CO_2 uptakes below 3 mmol/g at 0 °C and 1 bar. In the case of hydrogen adsorption, graphene oxide without and with Fe_3O_4 nanoparticles adsorbed 1.7 and 2.1 wt% of H_2, respectively, at −196 °C and 760 mmHg [28]. Only few materials have been tested as potential C_6H_6 adsorbents; for example, activated saran-derived carbon showed C_6H_6 uptake up to 11.6 mmol/g at 20 °C and pressure close to the saturation vapor pressure [15].

5 Conclusions

Graphene-based composite materials were synthesized by using polypyrrole and graphene oxide precursors and activated with KOH and potassium citrate. The resulting samples showed high BET surface areas (1650–2800 m^2/g), large pore volumes (0.73–1.66 cm^3/g) as well as large micropore volumes (0.43–0.78 cm^3/g). The KOH activation at 700 °C produced the sample with highest surface area, which showed very high uptakes of hydrogen (11.3 mmol/g at −196 °C and 760 mmHg) and benzene (15.8 mmol/g at 20 °C and relative pressure close to unity). As expected, the best CO_2 adsorption (6.8 mmol/g at 0 °C and 760 mmHg) was recorded for the most microporous sorbent (92%), which was obtained by activation with potassium citrate. Our findings confirm that graphene-based composite sorbents exhibit a great potential for gas capture/storage applications.

Acknowledgements BS and JC acknowledge the National Science Centre (Poland) for support of this research under Grant UMO-2016/23/B/ST5/00532.

References

1. US Department Of Energy, Targets for onboard hydrogen storage systems for light-duty vehicles (2012). http://energy.gov/sites/prod/files/2015/01/f19/fcto_myrdd_table_onboard_h2_storage_systems_doe_targets_ldv.pdf. Accessed 11 May 2016

2. H. Furukawa, N. Ko, Y.B. Go, N. Aratani, S.B. Choi, E. Choi, A.O. Yazaydin, R.Q. Snurr, M. O'Keeffe, J. Kim, O.M. Yaghi, Science **329**, 424 (2010)
3. A.K. Mishra, S. Ramaprabhu, J. Mater. Chem. **22**, 3708 (2012)
4. N.P. Wickramaratne, M. Jaroniec, ACS Appl. Mater. Interfaces **5**, 1849 (2013)
5. A. Wahby, J.M. Ramos-Fernández, M. Martinez-Escandell, A. Sepúlveda-Escribano, J. Silvestre-Albero, F. Rodriguez-Reínoso, ChemSusChem **3**, 974 (2010)
6. M. Nandi, K. Okada, A. Dutta, A. Bhaumik, J. Maruyama, D. Derks, H. Uyama, Chem. Commun. **48**, 10283 (2012)
7. H. Oh, S. Maurer, R. Balderas-Xicohtencatl, L. Arnold, O.V. Magdysyuk, G. Schütz, U. Müller, M. Hirscher, Int. J. Hydrogen Energ. **42**, 1027 (2017)
8. A. Klechikov, G. Mercier, T. Sharifi, I.A. Baburin, G. Seifert, A.V. Talyzin, Chem. Commun. **51**, 15280 (2015)
9. A. Ganesan, M.M. Shaijumon, Micropor. Mesopor. Mater. **220**, 21 (2016)
10. J. Choma, M. Marszewski, L. Osuchowski, J. Jagiello, A. Dziura, M. Jaroniec, ACS Sustainable Chem. Eng. **3**, 733 (2015)
11. J. Deng, Y. You, V. Sahajwalla, R.K. Joshi, Carbon **96**, 105 (2016)
12. V. Chandra, S.U. Yu, S.H. Kim, Y.S. Yoon, D.Y. Kim, A.H. Kwon, M. Meyyappan, K.S. Kim, Chem. Commun. **48**, 735 (2012)
13. M. Saleh, V. Chandra, K.C. Kemp, K.S. Kim, Nanotechnology **24**, 255702 (2013)
14. F.Q. Liu, W. Li, J. Zhao, W.H. Li, D.M. Chen, L.S. Sun, L. Wang, R.X. Li, J. Mater. Chem. A **3**, 12252 (2015)
15. A. Dziura, M. Marszewski, J. Choma, L.K.C. de Souza, L. Osuchowski, M. Jaroniec, Ind. Eng. Chem. Res. **53**, 15383 (2014)
16. M. Wiśniewski, S. Furmaniak, P. Kowalczyk, K.M. Werengowska, G. Rychlicki, Chem. Phys. Lett. **538**, 93 (2012)
17. G. Liu, M. Wan, Z. Huang, F. Kang, New Carbon Mater. **30**, 566 (2015)
18. European Union, Air quality standards (2016), http://ec.europa.eu/environment/air/quality/standards.htm. Accessed 20 May 2017
19. J. Choma, L. Osuchowski, A. Dziura, M. Marszewski, M. Jaroniec, Adsorpt. Sci. Technol. **33**, 587 (2015)
20. W.S. Hummers, R.E. Offeman, J. Am. Chem. Soc. **80**, 1339 (1958)
21. D.C. Marcano, D.V. Kosynkin, J.M. Berlin, A. Sinitskii, Z. Sun, A. Slesarev, L.B. Alemany, W. Lu, J.M. Tour, ACS Nano **4**, 4806 (2010)
22. L. Stobinski, B. Lesiak, A. Malolepszy, M. Mazurkiewicz, B. Mierzwa, J. Zemek, P. Jiricek, I. Bieloshapkad, J. Electron Spectrosc. **195**, 145 (2014)
23. J. Jagiello, J.P. Olivier, Carbon **55**, 70 (2013)
24. J. Jagiello, J.P. Olivier, Adsorption **19**, 777 (2013)
25. S. Brunauer, P.H. Emmett, E. Teller, J. Am. Chem. Soc. **60**, 309 (1938)
26. S. Chowdhury, R. Balasubramanian, J. CO_2 Util. **13**, 50 (2016)
27. Z.Y. Sui, Y.N. Meng, P.W. Xiao, Z.Q. Zhao, Z.X. Wei, B.H. Han, ACS Appl. Mater. Interfaces **7**, 1431 (2015)
28. S.E. Moradi, Appl. Phys. A **119**, 179 (2015)